Supramolecular self-organization in constitutional hybrid materials†

Simona Mihai, Adinela Cazacu, Carole Arnal-Herault, Gihane Nasr, Anca Meffre, Arie van der Lee and Mihail Barboiu*

Received (in Montpellier, France) 14th April 2009, Accepted 4th September 2009
First published as an Advance Article on the web 25th September 2009
DOI: 10.1039/b908641m

We present in this paper a new strategy to transcribe the supramolecular dynamic self-organization of the G-quadruplex and ureidocrown ether ion channel-type columnar architectures in constitutional hybrids. In particular, the use of a "*dynamic reversible hydrophobic interface*" can render the emerging hybrid mesophases self-adaptive. The reversible hydrophobic interactions allow both supramolecular and inorganic silica components to mutually (synergistically) adapt their spatial constitution during simultaneous (collective) formation of micrometric self-organized hybrid domains. More generally, applying such consideration to materials, leads to the definition of *constitutional hybrid materials*, in which organic (supramolecular)/inorganic domains are reversibly connected. This might provide new insights into the features that control the design of functional materials.

1. Introduction

Convergent multidimensional self-assembly of molecular components has been extensively used during the last few decades for the synthesis of functional supramolecular devices.[1] Kinetic or thermodynamic resolutions,[2,3] self-assembly followed by covalent modification,[4] and crystallization[5,6] shed light on useful strategies to control and to make convergence between self-organization and supramolecular functions. In this context, connecting the self-assembly processes with further covalent sol–gel modification might be considered as one straightforward approach used for the design of functional hybrid materials.[5–7] Considerable challenges still lie ahead and the more significant one is the "dynamic marriage" between supramolecular self-assembly and the sol–gel process. Both supramolecular and inorganic polymerization processes might "correlate" in order to converge towards self-organized nanomaterials. By using silsesquioxane precursors (Scheme 1) in which the functional organic and siloxane moieties are covalently connected during the sol–gel process, the weak supramolecular interactions positioning of the molecular components are typically less robust and they usually are destabilized when the cross-linked covalent siloxane network forms. The resulting hybrid architectures lead, in general, to amorphous or polymorphic materials.[7] One solution to overcome these difficulties is to improve the binding efficiency of molecular components. An increased number of interactions between molecular components may improve the stability of the templating supramolecular systems within the inorganic siloxane network. Numerous successful examples, pioneered by Shinkai *et al*. concern the use of organogels acting as robust templates during the tetraethoxysilane (TEOS) sol–gel process.[7d] We have recently reported nucleobase-based hybrids obtained under thermodynamic control.[4d] A second strategy presented in this paper is to use a reversible non-covalent interface between the supramolecular/organic and the siloxane/inorganic constituents. As the self-organization of organic/inorganic domains has to explore the hypersurface of all structure/energy combinations,[1] the build-up of final hybrid material upon a growing/self-reparation/termination sequence might be able to select the correct spatial geometries for the supramolecular organic and inorganic entities emerging from a collection of building blocks. A dynamic reversible interface might mediate the structural self-correlation of supramolecular and inorganic domains by virtue of their basic constitutional behaviours. The resulting hybrid material might undergo continual change in its constitution, through dissociation/reconstitution of different mesophases during the sol–gel process. This concept can be related to a sort of "*Chemical collectivism*" of colloidal systems, as described some years ago by Menger.[3a] Convergently, the self-replicating molecular and "dynablock" systems very recently described by Giussepone *et al*.[3b,c] are characterized by their aptitude to continuously organize at the macroscopic level the generation of their own components, when different blocks form in coupled equilibria. The reversibility of the interactions between components of a hybrid material might be a crucial factor and accordingly, a dynamic reversible hydrophobic interface might render the emergence of organic/inorganic mesophases self-adaptive, which mutually (synergistically) may adapt their 3D spatial distribution based on their own structural constitution during the simultaneous formation of hybrid self-organized domains.

In this context, we will present in this paper two examples of such constitutional hybrid materials prepared under thermodynamic control, containing supramolecular ion channel-type architectures combined with hydrophobic siloxanes as precursors for the inorganic silica matrix:

Institut Europeen des Membranes, ENSCM/UMII/UMR CNRS 5635, IEM/UMII, Place Eugene Bataillon CC047.
E-mail: mihai.barboiu@iemm.univ-montp2.fr;
Fax: (+33) 4 67 14 91 18
† Electronic supplementary information (ESI) available: Supplementary FTIR, NMR and powder XRD data. See DOI: 10.1039/b908641m

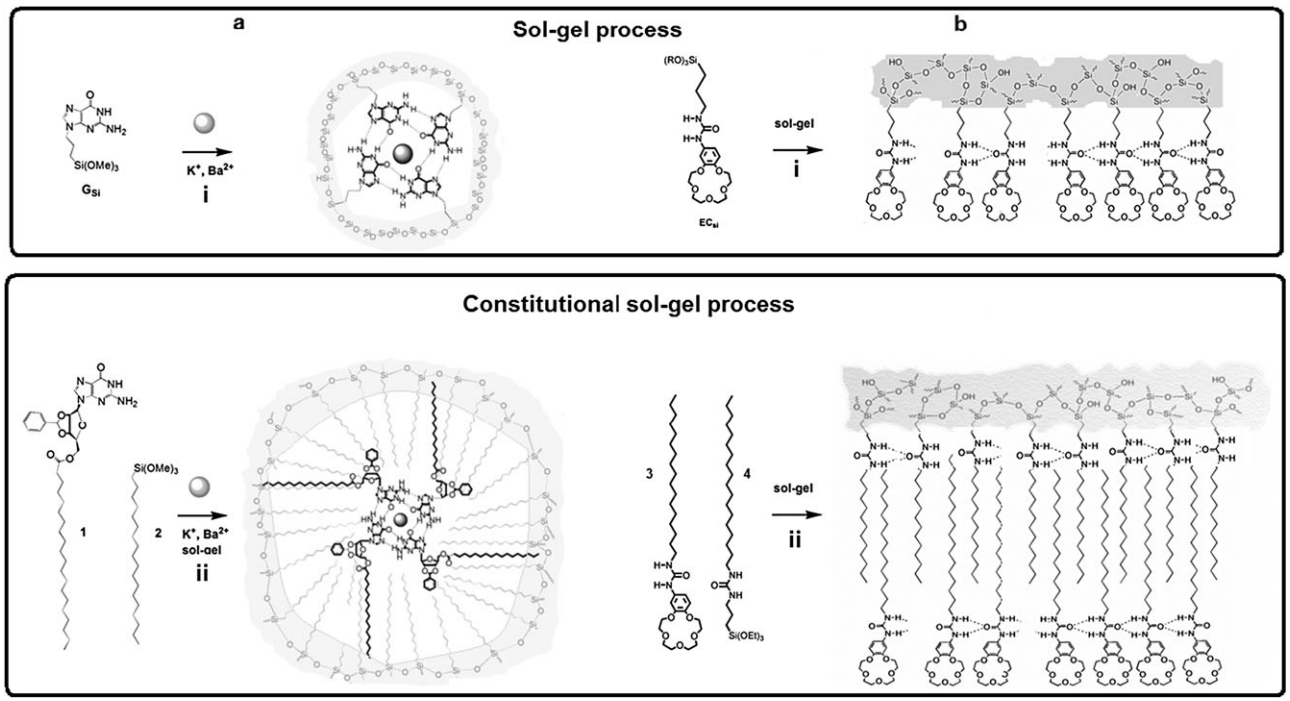

Scheme 1 Sol–gel process of (i) classical and (ii) constitutional hybrid materials based on (a) G-quadruplex and (b) ureidocrown ether architectures.

(a) The G-quartet, the hydrogen-bonded macrocycle formed by the self-assembly of guanosine, is stabilized by alkali cations.[8] (Scheme 1a) The role of cation templating is to stabilize by coordination to the eight carbonyl oxygens of two sandwiched G-quartets, the G-quadruplex, the columnar device formed by the vertical stacking of four G-quartets.

It represents a dynamic supramolecular system, in equilibrium with linear oligomers. New strategies using reversible polymerization or phase-change-driven selection were successfully used to generate G-quadruplex nanostructures.[8] We have recently reported a sol–gel route for preparing G-quadruplex-hybrids[4a] or dynameric membranes.[4b]

(b) The heteroditopic ureidocrown ethers[9a] complexing both cations and anions, and self-organizing into columnar oligomeric superstructures in solution and the solid state (Scheme 1b). Their self-organization in the liquid[9b] or bilayer membranes[9c] provided evidence for a hybrid carrier/channel transporting mechanism. Furthermore, these dynamic systems have been ''frozen'' in a hybrid matrix by a sol–gel process, transcribing their dynamic columnar self-organization in solid dense hybrid nanomembranes.[9d]

2. Experimental section

2.1 Materials and methods

Guanosine, benzaldehyde stearoyl chloride, octadecylisocyanate, octadecyltrimethoxy-silane (**2**), (triethoxysilyl)propan-1-amine and 4′-aminobenzo-15-crown-5 were purchased from Aldrich. $\mathbf{G_{Si}}$[4a] and $\mathbf{EC_{Si}}$[9d] were synthesised as previously reported. ^{1}H NMR and ^{13}C NMR spectra were recorded on an ARX 300 MHz spectrometer in $CDCl_3$ and DMSO-d_6 with the use of the residual solvent peak as reference. ^{29}Si MAS NMR was performed on a Brucker ASX400 spectrometer. Mass spectrometric studies (60 °C, cone voltage of V_c = 5–10 V) were performed by using a quadrupole Micromass, Platform II. Samples were introduced through a Waters 616HPLC pump. Solid state X-ray powder diffraction experiments were performed with Cu-Kα radiation at 20 °C using a Philips X'Pert Diffractometer equipped with an Xcelerator detector. CD spectra (220–400 nm) were collected on a MOS-450/AF-Biologic-CD spectrometer with a rate of 0.5 nm per step, using 10 mm quartz cells, at 25 °C. The measurements were carried out on $CHCl_3$ solutions (5×10^{-4} M of **2**) and on mixtures of **1**/**2** (1 : 1 and 1 : 2 mol/mol) briefly ultrasonicated with K^+ and Ba^{2+} ions (0.25 or 1 eq.).

2.2 General procedure for synthesis of compounds 1* and 1

9-(2′,3′-*O*-Benzylidene-β-D-ribofuranosyl)-guanine, 1*. Guanosine (5.0 g, 17.65 mmol) was suspended in benzaldehyde (50 ml) and dry zinc chloride (13.25 g, 97.18 mmol) was added. The mixture was stirred at room temperature overnight. Then, diethyl ether was added to precipitate the product. The crude material was filtered off and washed with cold water. The crude solid as mixture of diastereoisomers was recrystallized from ethanol–water (3 : 1) to give a pale yellow product (84%). ^{1}H NMR (DMSO-d_6, 300 MHz) δ 10.65 (s, 1H); 7. 90 and 7.87 (2s, 1H); 7.42–7.35 (m, 5H); 6.46 (s, 2H); 6.11 and 5.94 (2s, 1H); 6.02 (2d, 1H); 5.31 (m, 1H); 5.06 (m, 2H); 4.23 (m, 1H); 3.55 (m, 2H). ^{13}C NMR (DMSO-d_6, 300 MHz): δ 156.70; 153.66; 150.69; 136.15; 136.08; 129.75; 126.80; 116.74; 106.51; 102.99; 88.32; 87.68; 86.55; 84.49; 84.34; 83.16; 82.36; 80.80; 61.66.

9-(2′,3′-*O*-Benzylidene-β-D-ribofuranosyl)-5′stearoyl guanine, 1. Compound **1*** (2.0 g, 5.36 mmol), as mixture of diastereoisomers, was dissolved in 40 ml of anhydrous dimethylformamide; then,

dimethylaminopyridine (0.2 g, 1.61 mmol) and triethylamine (1.63 g, 16.08 mmol) were added. After 10 min, stearoyl chloride (2.27 g, 7.5 mmol) was slowly added. The mixture was stirred at room temperature overnight. The crude mixture was removed by rotary evaporation and chloroform was added. The crude material was purified by flash chromatography on silica gel (gradient eluent $CHCl_3$–MeOH 8 : 2). The fractions were removed and the product was washed with methanol to give pale yellow product (89%). ^{1}H NMR (DMSO-d_6, 300 MHz) δ 10.71 (s, 1H); 7.88 (s, 1H); 7.55–7.44 (m, 5H); 6.53 (s, 2H); 6.19 (s, 1H); 6.12 and 6.02 (2s, 1H); 5.41–5.31 (m, 2H); 4.48–4.18 (m, 3H); 2.26 (m, 2H); 1.47 (m, 2H); 1.23 (m, 28H); 0.84 (t, 3H). ^{13}C NMR (DMSO-d_6, 300 MHz): δ 174.94; 159.11; 153.68; 149.83; 135.02; 129.44; 128.14; 126.15; 115.92; 107.16; 103.73; 91; 90; 62.62; 33.83; 31.22; 22.20; 13.63.

2.3 General procedure for synthesis of A_K^+–D_K^+, A_{Ba}^{2+}–D_{Ba}^{2+} and the reference E hybrid materials

In typical run, 1 equiv. of octadecyltrimethoxysilane (**2**) and variable amounts of compound **1** together with the templating metal salt (see the ESI, Table 1S†) were dissolved in chloroform–acetone (1 : 0.25). 6 equiv. of deionized water and 3 equiv. of benzylamine (as catalyst) were added. Mixtures were stirred at 60 °C for 24 h and then the samples were slowly evaporated at room temperature to give sticky brown products, which were isolated and characterized. A second series of hybrids A_K^+–D_K^+, A_{Ba}^{2+}–D_{Ba}^{2+}, **E** were thermally treated at 90 °C for 24 h. A reference sol–gel sample, **E**, was prepared in the absence of salt triflates, under the same reaction conditions.

2.4 General procedure synthesis of compounds 3 and 4

4-Octadecylurea-benzo-15-crown-5, **3**, was prepared by refluxing 0.27 g (0.92 mmol) of octadecylisocyanate and 0.2 g (0.71 mmol) of 4′-aminobenzo-15-crown-5 (1.5 : 1 mol/mol) in acetonitrile (12 h). The crude product was recrystallized in hexane to afford, as a white powder, **3** (90% yield). ^{1}H NMR ($CDCl_3$, ppm) δ 0.88 (t, 3H, CH_3), 1.29 (m, 30H, CH_2), 1.49 (m, 2H, CH_2), 3.16 (m, 2H, CH_2), 3.75 (m, 8H, –O–CH_2–CH_2–O–), 3.90 (m, 4H, –O–CH_2–CH_2–O–), 4.11 (m, 4H, –O–CH_2–CH_2–O–), 4.70 (t, 1H, NH-Alkyl), 6.17 (s, 1H, NH-Aryl), 6.68 (dd, 1H), 6.82 (d, 1H), 6.95 (d, 1H). ^{13}C NMR ($CDCl_3$ ppm) δ 13.62, 22.19, 26.44, 28.87, 29.21, 29.68, 30.44[3], 31.42, 39.87, 68.13, 68.82, 69.95, 70.36, 108.58, 114.40, 122.90, 131.98, 145.66, 149.11, 156.04, 206.54. ES-MS: m/z (%): 601.62 (100) M + Na^+.

Octadecylureidopropyltrimethoxysilane, **4**, was prepared by refluxing 0.2 g (0.675 mmol) octadecylisocyanate and 0.179 g (0.811 mmol) of (triethoxysilyl)propan-1-amine in chloroform (12 h). The solvent was evaporated and the crude product was recrystallized in hexane to afford, as a white powder, **4** (82% yield). ^{1}H NMR ($CDCl_3$, ppm) δ 0.84 (m, 2H, αCH_2–Si–O–), 0.96 (m, 3H, CH_3 terminal), 1.16 (m, 2H, βCH_2–Si–O–), 1.22 (m, 6H, –Si–OR), 1.26 (m, 30H, CH_2), 1.33 (m, 2H, αCH_3 terminal), 3.24 (m, 2H, CH_2–NH 1et m, 2H, CH_2–NH_2), 3.83 (m, CH_3, –Si–OR), 3.98 (d, 1H, NH 1), 4.24 (d, 1H, NH 2); ^{13}C NMR ($CDCl_3$ ppm) δ 7.5, 14.1, 11.4, 22.9, 24.8, 26.4, 29.4, 29.6, 29.7, 31.9, 42.5, 45.7, 58.4, 157.7; ES-MS: m/z (%): 531.45 M + H^+.

2.5 General procedure for synthesis of A_i–B_i hybrid materials

i = 0, 10, 20, 40, 50, 60, 80% w/w can be achieved by mixing compounds **3** and **4** in acetone (ESI, Table 1S†), followed by the sol–gel process performed for 7 d at room temperature and using 6 equiv. of deionized water and 4 N HC for hybrid materials $\mathbf{A_i}$, and 3 equiv. of benzylamine for hybrid materials $\mathbf{B_i}$ as catalysts (ESI, Table 2S†). The sols were briefly stirred and allowed to react at room temperature under static conditions for 1 week and then samples were slowly evaporated at room temperature to give hybrid materials as white powders.

3. Results and discussion

3.1. Constitutional G-quadruplex hybrid materials

3.1.1 Design of hybrid molecular components. The lipophilic stearoyl guanosine, **1**, was prepared in two steps: the furanose protection with benzaldehyde leading to acetal **1*** as an equimolar diastereoisomeric mixture,[10a] followed by the reaction with stearyl chloride, to afford compound **1** as a white powder. The ^{1}H and ^{13}C NMR, and ESI-MS spectra are in agreement with the proposed formula.

^{1}H NMR experiments in d_6-DMSO indicated low defined self-association of "monomeric" **2**, as previously reported.[8] ^{1}H NMR spectra of mixtures **1**/K^+ and **1**/Ba^{2+} in $CDCl_3$ consist of broadened signals over temperatures from −60 °C to 50 °C, corresponding to fast interexchanging species in solution at the NMR time scale. The NMR signal of exchangeable NH^1 protons is broadened into the baseline at around δ 9.5–10.5 ppm (ESI, Fig. 1S†). After equilibration with K^+ or Ba^{2+}, the ^{1}H NMR spectrum in $CDCl_3$ presented sharp resonances for NH^1 amide protons (δ 9.9 and 10.06 ppm) and for NH^2 amine protons (δ 8.7 ppm), together with still present broad signals (ESI, Fig. 1S†). The fast exchange in solution was confirmed by the NOESY spectrum of such mixtures, which did not show clear NOEs between NH^1 and the H^8, as previously observed by Davis *et al.*[8l]

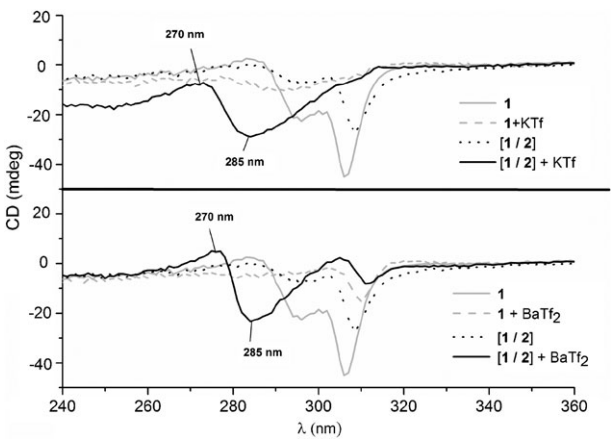

Fig. 1 The CD spectra at room temperature in $CHCl_3$ of lipophilic guanosine **1** (gray line), **1** + KOTf or **1** + $BaOTf_2$ (gray dashed line); mixture of **1**/**2** (black dotted line) and mixtures of **1**/**2** + KOTf or of **1**/**2** + $BaOTf_2$ (black line).

Next, we used CD spectroscopy to gain evidence that **1** forms G-quadruplex structures in the presence of ions in $CHCl_3$ (Fig. 1). In accordance with the NMR results, no active CD bands specific to a G-quadruplex were observed when **1** was mixed with ionic salts (KOTf and $BaOTf_2$) or with compound **2**, indicating that the G-quadruplex is either unstructured or exchanging very fast in solution. However, the observed CD spectra of such mixtures presented strong negative active CD bands at 295 and 305 nm as consequence of equilibrium between the two diastereoisomers in solution.[10a,b] Interestingly, mixtures of **1** with hydrophobic compound **2** (1 : 1 and 1 : 2 mol/mol) equilibrated with K^+ and Ba^{2+} ions gave the CD signature of a G-quadruplex with a positive band at λ = 270 nm and a negative band at λ = 285 nm, closely resembling the previously calculated CD spectra by Gray *et al.*[10c] of G-quadruplexes whose adjacent G-quartets have opposite polarities.

The stabilization of G-quadruplex structures in a hydrophobic environment occurred in a similar manner to that already observed in a hydrophobic environment, such as phospholipid liposomes.[8i,k,11] Having shown that mixtures of **1**/**2** equilibrated with K^+ and Ba^{2+} ions form G-quadruplex superstructures, we next evaluated their ability to form higher order superstructures in the solid state, by using *a sol–gel selection process*.[4a] The generation of *G-quadruplex hybrid materials* $\mathbf{A_K}^+$–$\mathbf{D_K}^+$ or $\mathbf{A_{Ba}}^{2+}$–$\mathbf{D_{Ba}}^{2+}$ can be achieved by mixing guanosine stearoyl derivative, **1**, and octadecyltrimethoxysilane, **2**, compounds with potassium or barium triflates in chloroform/acetone, followed by the sol–gel process performed at 60 °C and using benzylamine as catalyst (Scheme 1a and ESI, Table 1S†). We also carried out sol–gel process, in the absence of K^+ or Ba^{2+} cations, resulting in the formation of a *G-hybrid material*, **E**. A portion of these materials were then dried at 90 °C for 24 h in order to achieve complete condensation of inorganic siloxane network.

3.1.2 Spectroscopic and X-ray diffraction characterization of G-quadruplex hybrid materials. FTIR and NMR spectroscopic analyses demonstrate the formation of a self-organized organic–inorganic network. FTIR spectra of hybrid materials show the appearance of the broad vibrations of $\nu_{Si-O-Si}$ = 900–1200 cm^{-1} instead of the vibrations ν_{Si-OEt} = 950, 1070 and 1100 cm^{-1} initially observed for the molecular precursor, **2**. Evidence for H-bonding and K^+ complexation was obtained from the vibration shifts of the –C=O bonds, detected after hydrolysis–condensation reactions: $\nu_{C=O}$ = 1737–1699 cm^{-1}. This demonstrates that the self-organization is preserved in the hybrid materials throughout the sol–gel polymerization process (ESI, Fig. 3S and 4S†). ^{29}Si MAS NMR spectroscopic experiments are in agreement for both $\mathbf{A_K}^+$–$\mathbf{D_K}^+$ and $\mathbf{A_{Ba}}^{2+}$–$\mathbf{D_{Ba}}^{2+}$, and the reference **E** hybrid materials, with a partially condensed hybrid material (61.3%), with a lower percentage of cross-linked T^3 C–$Si(OSi)_3$ (8%) units, and mostly composed of T^1 C–$Si(OSi)(OH)_2$ (24%) and T^2 C–$Si(OSi)_2(OH)$ (68%) units, showing a predominant 2D arrangement.

This indicates that the self assembly processes occurs differently in the presence or in the absence of K^+ templating ions, and seems to not influence the hydrolysis–condensation reactions of the alkoxysilane groups during the sol–gel process. ^{29}Si MAS NMR spectroscopic experiments are in agreement with the ~100% T^3 C–$Si(OSi)_3$ units, corresponding to a totally condensed silica matrix in hybrid materials **A–E** after the thermal treatment.

Further valuable insights into the self-organization of $\mathbf{A_K}^+$–$\mathbf{D_K}^+$ or $\mathbf{A_{Ba}}^{2+}$–$\mathbf{D_{Ba}}^{2+}$ and reference **E** hybrid materials were obtained by X-ray powder diffraction (powder XRD).

Firstly, the powder XRD patterns of lipophilic guanosine **1** derivative, equilibrated with salts (Na^+, K^+, Ba^{2+}) display broad peaks and the presence of the Bragg diffraction peak at 2θ = 26.8° (d = 3.41 Å) is representative for the π–π stacking distance between two planar G-quartets (ESI, Fig. 5S†).[4a,b] The XRPD patterns of the both *G-quadruplex hybrids* $\mathbf{A_K}^+$–$\mathbf{D_K}^+$ and $\mathbf{A_{Ba}}^{2+}$–$\mathbf{D_{Ba}}^{2+}$ presents well-resolved peaks. An indexation was attempted for several observed powder diffraction diagrams (Fig. 2).

For $\mathbf{D_K}^+$ (Fig. 2a,c), all peaks could be indexed with a monoclinic unit cell of a = 15.35, b = 4.14, c = 23.97 Å, β = 94.01°, possible space groups $P2$ or $P2_1$ (in the latter case the b parameter should be doubled, the quality of the diffractogram does not allow the two cases to be distinguished). With a unit cell volume of 1520 $Å^3$, the independent molecule in the asymmetric unit is expected to contain 40–45 non-H atoms, slightly less than the 48 atoms of **1**. In the case of a doubled b-parameter, and hence a double cell volume, the asymmetric unit of the unit cell incorporates 84 non-H atoms, which is very close to the 81 independent atoms of the complete hybrid material of **1** and **2** combination and which is thus more logic than the first hypothesis.

The diagrams in Fig. 2b,d corresponding to $\mathbf{A_{Ba}}^{2+}$–$\mathbf{D_{Ba}}^{2+}$ are easily indexed on the basis of a repeat unit of approximately 48 Å between the individual stacks. This feature was not observed for the XRPD patterns of the non-templated *G-hybrid* material, **E** (Fig. 2, **E** patterns).

It is noted that the crystallinity of the Ba^{2+}-templated materials is extremely high compared with the K^+-templated analogs, in view of the harmonic signal peaks, indicative of long-level structured material.[12] A comparison between the K^+- and the Ba^{2+}-templated hybrid materials thus shows that the second is lamellar in nature with a high crystallinity in the stacking direction, and that the first is more three-dimensional in nature with a somewhat lower crystallinity.

We believe that in the first sol–gel step, the G-quadruplexes are fixed *via* the hydrophobic interface in the siloxane network of **2**. These fixed ("*frozen*") objects highly self-correlate, as proven by powder XRD experiments, to generate anisotropic mesophases interconnected *via* condensed lipophilic siloxane bridges. With increasing amounts of **2**, the observed peaks are less well-defined and the peak width increases, indicating smaller domains in which coherent scattering occurs (Fig. 2c,d). After the thermal treatment and the complete condensation of the siloxane network, the crystallinity greatly decreases. The peak at 2θ = 26.7° (d = 3.3 Å) and representative for the π–π stacking distance between two planar G-quartets, is amazingly amplified (ESI, Fig. 6S†).

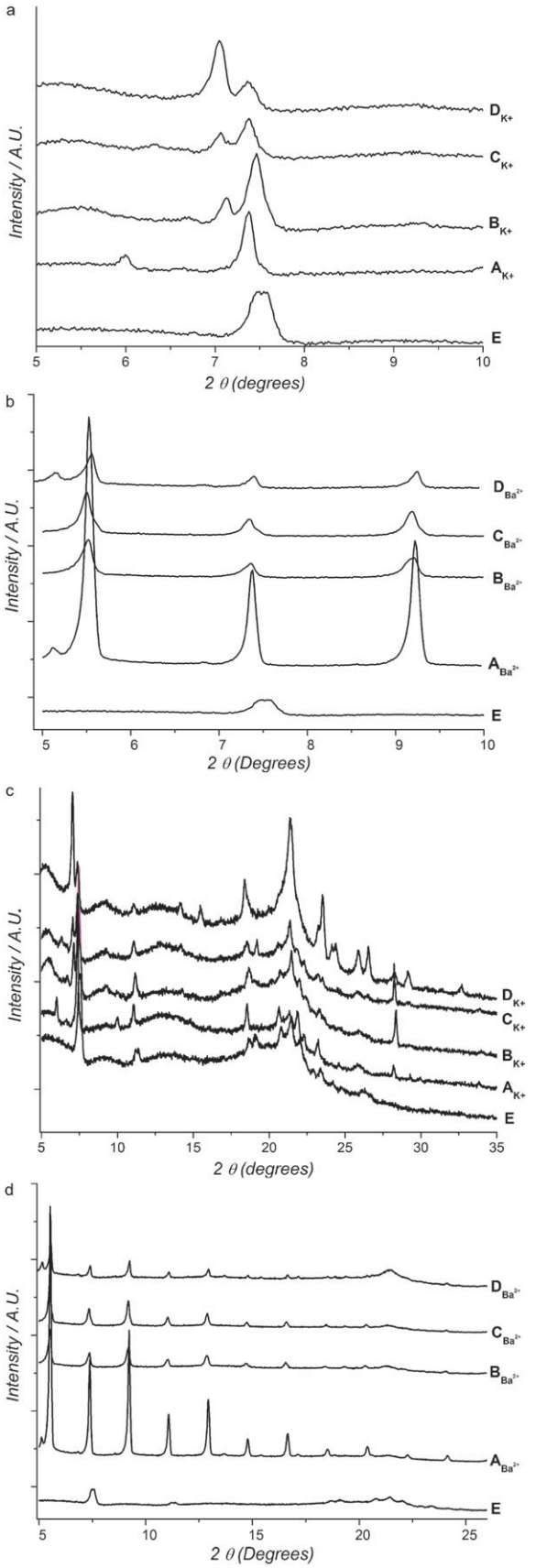

Fig. 2 Powder XRD patterns of hybrids **A–E** templated in the presence of KOTf: (a) low and (c) high angles and of $BaOTf_2$: (b) low and (d) high angles.

3.2 Constitutional ureidobenzocrown ether hybrid materials

3.2.1 Design of hybrid molecular components 3 and 4. Our efforts also involved the synthesis of *constitutional hybrids* based on octadecylureido-15-crown-5 derivative **3**, and octadecylureido-propyltrimethoxysilane **4** (Scheme 1b). For structural (H-bonding and packing presented below) reasons, both hybrid components have been designed bearing an urea moiety. The octadecylisocyanate was treated with the aminobenzo-15-crown-5 and 3-(triethoxysilyl)propan-1-amine, (CH_3CN, Δ, 5h) to afford, after crystallization, **3** and **4**, respectively, as white powders (90%). The ^1H and ^{13}C NMR, and ESI-MS spectra are in agreement with the proposed formula.

3.2.2 Spectroscopic and powder XRD characterization of ureidocrown ether hybrid materials, A_i and B_i, i = 0–80. The FTIR spectra of hybrid materials $\mathbf{A_i}$ and $\mathbf{B_i}$ showed the appearance of broad vibrations of the $\nu_{Si-O-Si}$ = 1110–1125 cm^{-1} instead of the vibrations ν_{Si-OEt} = 950, 1070, 1100 cm^{-1}, initially observed for the molecular precursor **4**. Evidence for strong urea H-bonding was obtained from the FTIR spectra of solids $\mathbf{A_i}$ and $\mathbf{B_i}$; the H-bond vibration shifts of the urea moiety were detected: ν_{N-H} = 3310 ($\Delta\nu$ = 30), $\nu_{C=O}$ = 1630 ($\Delta\nu$ = 15) and ν_{C-N} = 1570 ($\Delta\nu$ = 25) cm^{-1}.[6] Moreover, we observed a widening of the ν_{N-H} = 3300 cm^{-1} vibration band, resulting from superposition of several signals. ^{29}Si MAS-NMR spectroscopic experiments were in agreement with the almost complete 3D condensed $\mathbf{A_i}$ materials (~95 % T^3 C–$Si(OSi)_3$) and with the 2D condensed $\mathbf{B_i}$ materials (~70–90%). The $\mathbf{B_i}$ materials only presented a lower percentage of T^3 C–$Si(OSi)_3$ (8%) and were mostly composed of T^2 C–$Si(OSi)_2$ (OH) (20–80%) and T^1 C–$Si(OSi)(OH)_2$ (15–80%) units. Moreover, by increasing the amounts of templating self-organized macrocycle **3**, we observed an increase in the amounts of T^2 units in the $\mathbf{B_i}$ materials (ESI, Table 3S†). We presume that the hydrolysis–condensation reactions of the siloxane network correlate with a linear self-organization of **1** during the sol–gel process. We have previously shown[9] that in solution, the ureidocrown

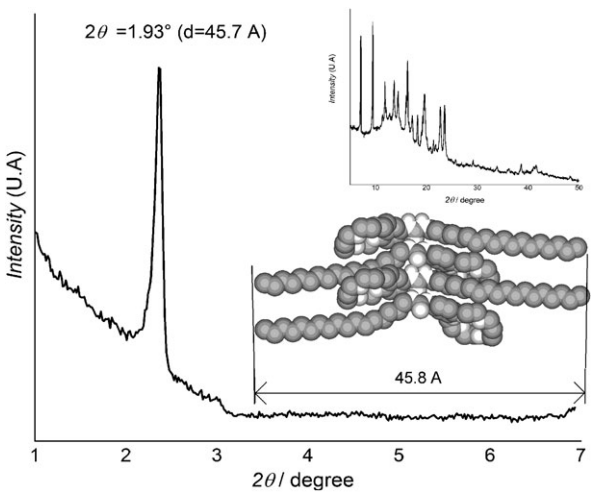

Fig. 3 Low angle powder XRD patterns of 4-octadecylurea-benzo-15-crown-5, **3** (high angle powder XRD in detail).

ethers form at least two types of hydrogen-bonded aggregates that can be modelled as a dimer followed by discrete higher oligomers. In the solid state, the macrocyclic compound **3** adopts a preferential *anti-parallel columnar packing* in the solid state (Fig. 3).[9c]

For a similar hexylureabenzocrown ether compound, it was possible to obtain full atomic structure determination and to generate the corresponding diffractogram using the data of single crystal measurements. By comparing the diffractogram generated from the single crystal structure solution with the experimental diffraction results of the bulk powder of **3** it can be seen that the preferential antiparallel dimeric packing co-exists with a second residual polymorph. It can be postulated that in the solid state, the *antiparallel packing* corresponding to the first intense peak is preferential to the residual *parallel packing* corresponding to the second small peak. Fig. 3 shows the powder XRD patterns of compound **3**. The diffraction pattern of **3** could be indexed using a monoclinic unit cell with $a = 37.65$, $b = 9.10$, $c = 9.25$ Å, $\beta = 97.71°$, $V = 3140$ Å^3, corresponding to 43–44 atoms in the asymmetric unit, and thus accommodating the 40 non-H atoms of **3** plus 3–4 atoms from either a solvent acetonitrile or disordered octadecyl unit (possibly situated between two unit cells). The first intense diffraction peak is related to the length of the molecule obtained by molecular modelling of the structures of these complexes on the basis of the geometry in the crystal structure, using a linear geometry for the alkyl substituents. The same premise was observed in the powder XRD patterns of precursor **3**.

The relative arrangement of **4** in the crystal of the anti-parallel H-bonded aggregates is similar to the previously described five single-crystal structures of different 3-(ureiodoarene)propyl-triethoxysilane superstructures;[4c] in the crystal lattice these compounds pack in one direction, into ureiodoarene and triethoxysilane layers.[4c] These layers, which are alternatively stratified, exhibit two types of interfaces in between: one contact surface due to the aromatic interactions and the other surface resulting from hydrophobic interactions of alkyl groups that are in van der Waals contact. Assuming that the octadecyl moieties are linear, interpenetrated layers of antiparallel H-bonded oligomers generate an architecture in

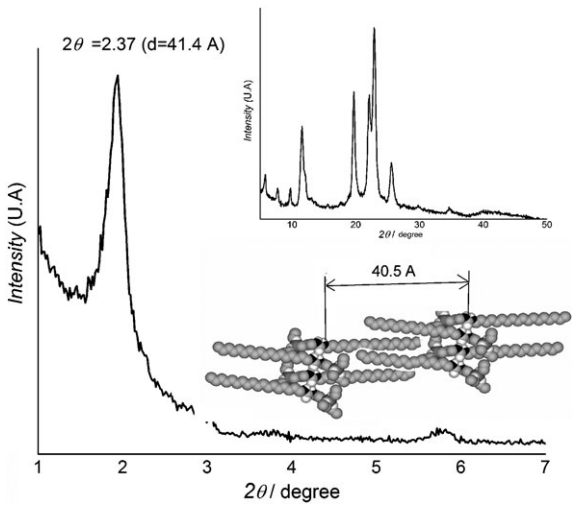

Fig. 4 Low angle powder XRD patterns of octadecylureidopropyl-trimethoxysilane, **4** (high angle powder XRD in detail).

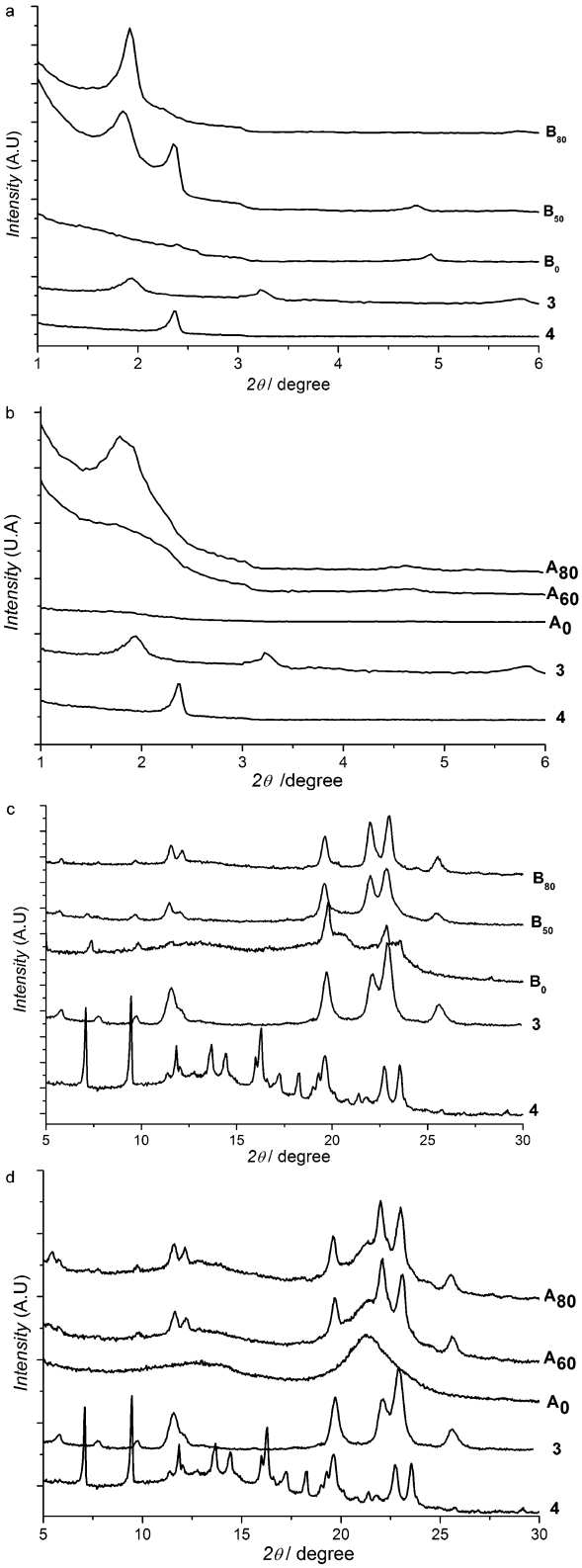

Fig. 5 Powder XRD patterns of compounds **3** and **4**, and hybrid materials $\mathbf{A_i}$ and $\mathbf{B_i}$, i = 0, 50, 60, 80% w/w prepared by using benzylamine (basic) catalyst: (a) low and (b) high angles and HCl (acidic) (c) low and (d) high angles.

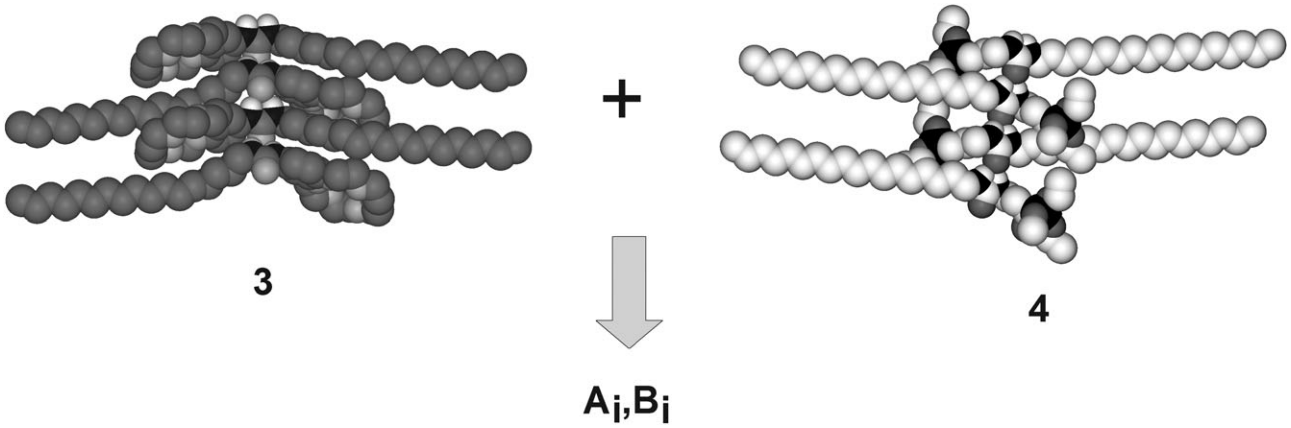

Scheme 2 Schematic representation of mixture of patterns of macrocyclic compound **3** and hydrophobic siloxane **4** in self-organized hybrid materials $\mathbf{A_i}$ and $\mathbf{B_i}$.

which the distance between urea ribbons of $(\mathbf{4})_n$ anti-parallel H-bonded oligomers is compatible with the distance corresponding to the first intense diffraction peak at $2\theta = 2.37^\circ$ ($d = 41.4$ Å) (Fig. 4).

Further valuable insights into the self-organization of $\mathbf{A_i}$ and $\mathbf{B_i}$ materials were obtained from the powder XRD (Fig. 5). After the sol–gel process, the powder XRD data shows that the long-range order of $\mathbf{A_i}$ and $\mathbf{B_i}$ hybrid materials is less pronounced than in the precursors **3** and **4**: there are less well-defined peaks present than for the precursors and the average peak width increases, indicating smaller domains in which coherent scattering occurs.

However, it was noted that the crystallinity of $\mathbf{A_i}$ and $\mathbf{B_i}$ materials is higher compared with the classical silsesquioxane-type hybrid materials,[4,7,9] in view of the more-defined signal powder XRD peaks. The $\mathbf{B_i}$ (base-catalysed) materials (Fig. 5a,c) are more structured than the $\mathbf{A_i}$ (acid-catalysed) analogs (Fig. 5b,d), in correlation with ^{29}Si MAS-NMR experiments. After increasing the amounts of **3**, from 10 to 50% w/w, the crystallinity of both $\mathbf{A_i}$ and $\mathbf{B_i}$ hybrids was not extremely high in view of the largeness of the diffraction peaks (ESI, Fig. 8S†). However, for the concentrations $c_1 > 50$ wt%, the observed powder XRD peaks are indicative of the self-organized columnar patterns of macrocyclic compound **3** (Fig. 5 $\mathbf{A_i}$ and $\mathbf{B_i}$ i = 60, 80). We believe that for the sol–gel step, a critical concentration of **3** (C > 50 wt%) is needed for increasing the density and the orientation of the columnar-packed architectures, which percolate in "highly concentrated" hybrid materials. These domains of dominant self-organization behaviour of **3** are fixed *via* the hydrophobic interfaces in the siloxane network of **4** (Scheme 2). The low-angle peaks in the range 1.0–6.0° are indicative of the long-range organization of the $\mathbf{A_{50-80}}$ and $\mathbf{B_{50-80}}$ hybrids. For $\mathbf{A_{50-80}}$ cross-linked hybrids, one diffraction peak is located at $2\theta = 1.8^\circ$ ($d = 46.8$ Å), indicating that the materials express a cross-over (mixed) behaviour of interfering networks of **3** and **4**.

The robustness/stability of superstructures of **3** and **4** is strongly expressed in an independent way (linear combination) in the hybrid structure of $\mathbf{B_{50}}$, presenting two distinct diffraction peaks at $2\theta = 1.85^\circ$ ($d = 46.82$ Å) and at $2\theta = 2.34^\circ$ ($d = 41.8$ Å), corresponding to the signature of a mixture of interpenetrated H-bonded networks of **3** and **4** (Fig. 5a,c, $\mathbf{B_{50}}$). Increasing the amount of **3** introduces a dominant behaviour

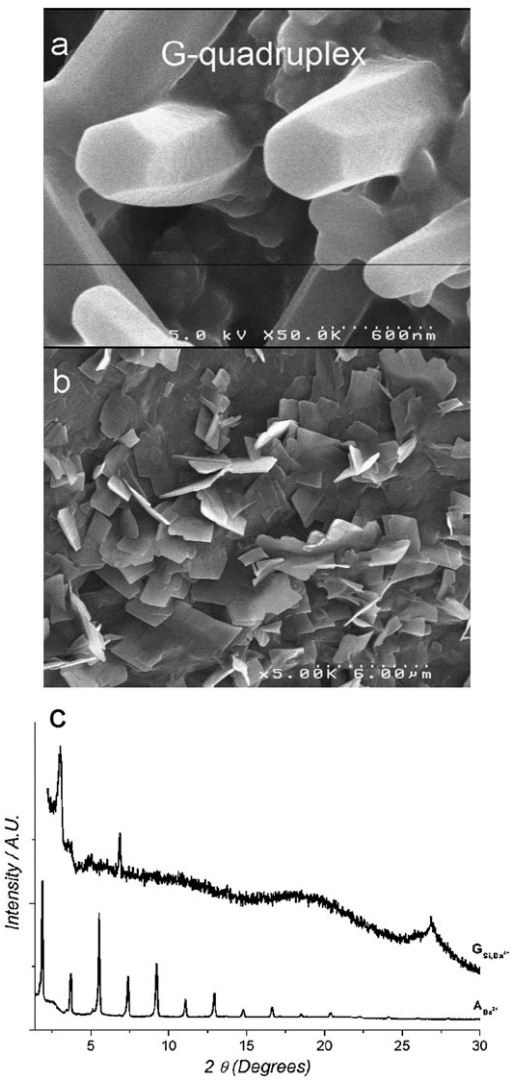

Fig. 6 (a,b) SEM images and (c) powder XRD patterns of (a) classical $(\mathbf{G_{Si}})_4\mathbf{K}^+$, and (b) of constitutional $\mathbf{A_{Ba}}^{2+}$ G-quadruplex hybrids.

in the structure of $\mathbf{B_{80}}$, such as the interpenetrated macrocyclic network imposing its own output over the other one (**4**), as only one peak at $2\theta = 1.85^\circ$ ($d = 46.82$Å) is present in powder XRD of this material (Fig. 5a,c, $\mathbf{B_{80}}$).

3.3 Comparative analysis of classical silsesquioxane and constitutional dynamic hybrid materials

The present results showed that highly self-organized materials can be synthesized by using a dynamic communicating interface between organic and inorganic hybrid mesophases. The last step of this work consists of comparing the novel "constitutional hybrid materials" with "classical covalent hybrids" previously reported by our group.[4a,9d] The remarkable G-quadruplex twisted hybrid nanorods can be obtained as previously reported[4a] at the nanometric level by using silsesquioxane $\mathbf{G_{Si}}$ under the experimental conditions reported in section 2.3 (Fig. 6a). These nanorods correlated with an ordered hexagonal structure with the Bragg diffraction peak at $2\theta = 3.0^\circ$ corresponding to a characteristic distance $d = 29.4$ Å, are compatible with the diameter of the hexagonal packed G-quartet superstructure.[4a] The $\mathbf{A_{Ba}}^{2+}$–$\mathbf{D_{Ba}}^{2+}$ and $\mathbf{A_K}^{+}$–$\mathbf{D_K}^{+}$ constitutional hybrids showed high organisation, with $a = 64.4$ Å for $\mathbf{A_K}^{+}$–$\mathbf{D_K}^{+}$ and $a = 47.2$ Å for $\mathbf{A_{Ba}}^{2+}$–$\mathbf{D_{Ba}}^{2+}$ compatible with octadecyl-G-quartet superstructures.

It seems that these materials are more structured than the classical $\mathbf{(G_{Si})_4K}^{+}$ analogs in view of the sharpness and the number of the diffraction peaks observed in XPRS patterns (Fig. 6c). Moreover, scanning electron microscopy (SEM) images of materials $\mathbf{A_{Ba}}^{2+}$–$\mathbf{D_{Ba}}^{2+}$ and $\mathbf{A_K}^{+}$–$\mathbf{D_K}^{+}$ show dense, compact solids with a micrometric plate-like morphology.

The same premises hold true for the ureido-crown ether hybrid systems $\mathbf{A_i}$ and $\mathbf{B_i}$ (Fig. 7). These constitutional hybrids are reaching a better level of organisation giving access to a large number of crystalline order in view of the higher number of diffraction peaks observed in powder XRD patterns $\mathbf{A_i}$ and $\mathbf{B_i}$ (Fig. 7c). Moreover, while the classical hybrids prepared from silsesquioxane $\mathbf{EC_{Si}}$[9b] under the same experimental conditions as described in section 2.5 are compact dense solids with a granular morphology (Fig. 7a), the constitutional hybrids $\mathbf{A_i}$ and $\mathbf{B_i}$ consist of crystalline rods of micrometric dimension. The organisation at micrometric length of both "hybrid constitutional materials" studied in this paper, compared with the classical ones showing nanometric organization, is probably dependent of the superior emergence of self-organizing collective domains adapting along the hydrophobic reversible interfaces. This may increase the size of self-organized domains, increasing the dimension of the resulting G-quadruplex and ureidocrown ether constitutional hybrids.

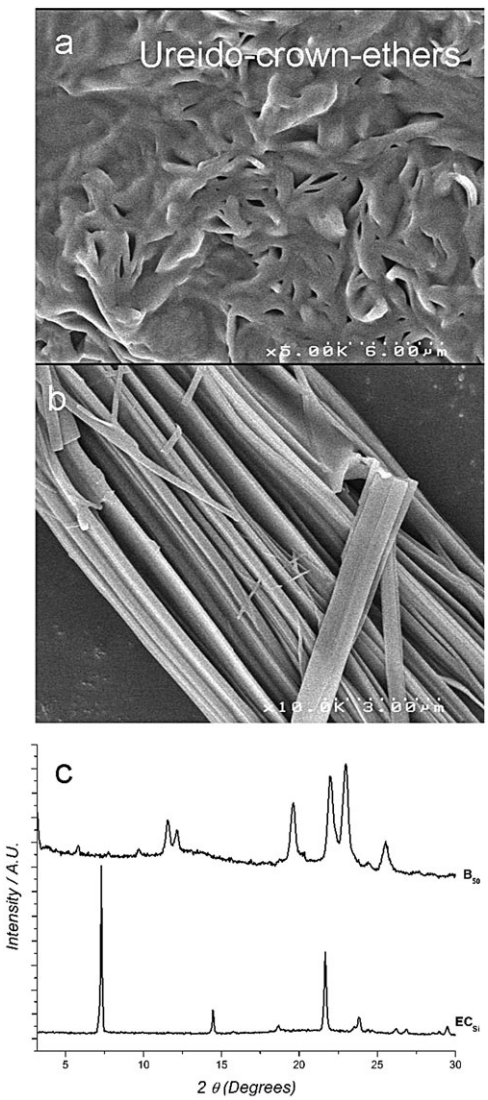

Fig. 7 (a,b) SEM images and (c) powder XRD patterns of (a) classical $\mathbf{EC_{Si}}$, and (b) of constitutional $\mathbf{B_{50}}$ ureidocrown ether hybrids.

4. Conclusions

In conclusion, the results presented here reveal a new strategy to transcribe and to fix the supramolecular ion channel-type architectures in self-organized constitutional hybrids. In particular, the use of a communicating hydrophobic interface between organic/supramolecular and inorganic/siloxane networks is noteworthy and represent a useful strategy for improving their compatibility. Interpenetrated hybrid components led after the sol–gel process to materials in which the features of the supramolecular and inorganic networks are expressed *via* cross-over and linear processing schemes. Dynamic self-assembly of supramolecular systems prepared under thermodynamic control may in principle be connected to a kinetically controlled sol–gel process (under basic catalysis), in order to extract and select the interpenetrated self-organized networks under a specific set of experimental conditions. Such "dynamic marriage" between supramolecular self-assembly and inorganic sol–gel polymerization processes that synergistically communicate, leads to higher self-organized hybrid materials with increased micrometric scales. More generally, applying such consideration to hybrid materials leads to the definition of *constitutional hybrid materials*, in which organic (supramolecular)/inorganic domains are reversibly connected. This might provide new insights into the basic features that control the design of functional constitutional architectures.[1] Considering the simplicity of this strategy, possible applications on the synthesis

of more complex hybrid architectures might be very effective, coming close to novel expressions of complex matter.

Acknowledgements

This work, conducted under the European Heads of Research Councils and European Science Foundation EURYI (European Young Investigator) Awards scheme in 2004, was supported by funds from the Participating Organizations of EURYI and the EC Sixth Framework Program. See http://www.esf.org/euryi.

Notes and references

1 (*a*) J.-M. Lehn, *Chem. Soc. Rev.*, 2007, **36**, 151–160; (*b*) J. A. Thomas, *Chem. Soc. Rev.*, 2007, **36**, 856–868.

2 (*a*) P. Vongvilai, M. Angelin, R. Larsson and O. Ramström, *Angew. Chem.*, 2007, **119**, 966–968 (*Angew. Chem., Int. Ed.*, 2007, **46**, 948–950); (*b*) R. Larsson and O. Ramström, *Eur. J. Org. Chem.*, 2006, 285–291; (*c*) R. Larsson, Z. Pei and O. Ramström, *Angew. Chem.*, 2004, **116**, 3802–3804 (*Angew. Chem., Int. Ed.*, 2004, **43**, 3716–3718); (*d*) M. Angelin, P. Vongvilai, A. Fischer and O. Ramström, *Chem. Commun.*, 2008, 768–770; (*e*) M. Angelin, P. Vongvilai, A. Fischer and O. Ramström, *J. Org. Chem.*, 2008, **73**, 3593–3595.

3 (*a*) F. Menger, *Angew. Chem.*, 1991, **103**, 1104–1118 (*Angew. Chem., Int. Ed. Engl.*, 1991, **30**, 1086–1089); (*b*) S. Xu and N. Giuseppone, *J. Am. Chem. Soc.*, 2008, **130**, 1826–1827; (*c*) R. Nguyen, L. Allouche, E. Buhler and N. Giuseppone, *Angew. Chem.*, 2009, **121**, 1113–1116 (*Angew. Chem., Int. Ed.*, 2009, **48**, 1093–1096) and references therein.

4 (*a*) C. Arnal-Hérault, M. Michau, A. Pasc-Banu and M. Barboiu, *Angew. Chem.*, 2007, **119**, 4346–4350 (*Angew. Chem., Int. Ed.*, 2007, **46**, 4268–4272); (*b*) C. Arnal-Hérault, A. Pasc-Banu, M. Michau, D. Cot, E. Petit and M. Barboiu, *Angew. Chem.*, 2007, **119**, 8561–8565 (*Angew. Chem., Int. Ed.*, 2007, **46**, 8409–8413); (*c*) M. Michau, M. Barboiu, R. Caraballo, C. Arnal-Hérault, P. Periat, A. van der Lee and A. Pasc, *Chem.–Eur. J.*, 2008, **14**, 1776–1783; (*d*) C. Arnal-Hérault, M. Barboiu, A. Pasc, M. Michau, P. Perriat and A. van der Lee, *Chem.–Eur. J.*, 2007, **13**, 6792–6800.

5 (*a*) P. N. W. Baxter, J.-M. Lehn and K. Rissanen, *Chem. Commun.*, 1997, 1323–1324; (*b*) M. Hutin, C. J. Cramer, L. Gagliardi, L. A. R. Shahi, G. Bernardinelli, R. Cerny and J. R. Nitschke, *J. Am. Chem. Soc.*, 2007, **129**, 8774–8780; (*c*) P. N. W. Baxter, J.-M. Lehn, G. Baum and D. Fenske, *Chem.–Eur. J.*, 2000, **6**, 4510–4517; (*d*) C. D. Pentecost, K. S. Chichak, A. J. Peters, G. W. V. Cave, S. J. Cantrill and J. F. Stoddart, *Angew. Chem.*, 2006, **119**, 222–226 (*Angew. Chem. Int. Ed.*, 2006, **45**, 218–222); (*e*) C.-F. Chow, S. Fujii and J.-M. Lehn, *Chem. Commun.*, 2007, 4363–4365.

6 (*a*) F. Dumitru, E. Petit, A. van der Lee and M. Barboiu, *Eur. J. Inorg. Chem.*, 2005, 4255–4262; (*b*) Y. M. Legrand, A. van der Lee and M. Barboiu, *Inorg. Chem.*, 2007, **46**, 9083–9089; (*c*) M. Barboiu, E. Petit, A. van der Lee and G. Vaughan, *Inorg. Chem.*, 2006, **45**, 484–486.

7 (*a*) C. Sanchez, H. Arribart and M. M. Girau-Guille, *Nat. Mater.*, 2005, **4**, 277–288; (*b*) J. J. E. Moreau, L. Vellutini, M. Wong Chi Man, C. Bied, J. L. Bantignies, P. Dieudonné and J. L. Sauvajol, *J. Am. Chem. Soc.*, 2001, **123**, 7957–7958; (*c*) R. J. P. Corriu, *Eur. J. Inorg. Chem.*, 2001, 1109–1121; (*d*) K. J. C. van Bommel, A. Frigerri and S. Shinkai, *Angew. Chem.*, 2003, **115**, 1010–1030 (*Angew. Chem., Int. Ed.*, 2003, **42**, 980–999); (*e*) M. Barboiu, C. Guizard, C. Luca, B. Albu, N. Hovnanian and J. Palmeri, *J. Membr. Sci.*, 1999, **161**, 193–206; (*f*) M. Barboiu, C. Guizard, C. Luca, N. Hovnanian, J. Palmeri and L. Cot, *J. Membr. Sci.*, 2000, **174**, 277–286; (*g*) M. Barboiu, C. Guizard, N. Hovnanian, J. Palmeri, C. Reibel, C. Luca and L. Cot, *J. Membr. Sci.*, 2000, **172**, 91–103; (*h*) O. Villamo, C. Barboiu, M. Barboiu, W. Yau-Chun-Wan and N. Hovnanian, *J. Membr. Sci.*, 2002, **204**, 97–110; (*i*) C. Guizard, A. Bac, M. Barboiu and N. Hovnanian, *Sep. Purif. Technol.*, 2001, **25**, 167–180.

8 (*a*) J. T. Davis and G. P. Spada, *Chem. Soc. Rev.*, 2007, **36**, 296–313; (*b*) J. T. Davis, *Angew. Chem.*, 2004, **116**, 684–716 (*Angew. Chem., Int. Ed.*, 2004, **43**, 668–698); (*c*) T. Giorgi, S. Lena, P. Mariani, M. A. Cremonini, S. Masiero, S. Pieracini, J. P. Rabe, P. Samori, G. P. Spada and G. Gotarelli, *J. Am. Chem. Soc.*, 2003, **125**, 14741–17479; (*d*) S. Pieraccini, S. Masiero, O. Pandoli, P. Samori, G. P. Spada and G. Gotarelli, *Org. Lett.*, 2006, **8**, 3125–3128; (*e*) A. Ghoussoub and J.-M. Lehn, *Chem. Commun.*, 2005, 5763–5765; (*f*) V. Setnička, M. Urbanová, K. Volka, S. Nampally and J.-M. Lehn, *Chem.–Eur. J.*, 2006, **12**, 8735–8743; (*g*) S. Nampally and J.-M. Lehn, *Chem.–Asian J.*, 2008, **3**, 134–139; (*h*) W. C. Dreive and S. Neidle, *Chem. Commun.*, 2008, 5295–5297; (*i*) M. S. Kaucher, W. A. Harrell and J. T. Davis, *J. Am. Chem. Soc.*, 2006, **128**, 38–39; (*j*) L. Ma, M. Iezzi, M. S. Kaucher, Y. F. Lam and J. T. Davis, *J. Am. Chem. Soc.*, 2006, **128**, 15269–15277; (*k*) L. Ma, M. Melegari, M. Collombini and J. T. Davis, *J. Am. Chem. Soc.*, 2008, **130**, 2938–2939; (*l*) M. S. Kaucher, Y. F. Lam, S. Pieraccini, G. Gotarelli and J. T. Davis, *Chem.–Eur. J.*, 2005, **11**, 164–163; (*m*) V. Shi, K. M. Mullaugh, J. C. Fettinger, Y. Jiang, S. A. Hofstadler and J. T. Davis, *J. Am. Chem. Soc.*, 2003, **125**, 10830–10841.

9 (*a*) M. Barboiu, G. Vaughan and A. van der Lee, *Org. Lett.*, 2003, **5**, 3073–3076; (*b*) M. Barboiu, *J. Inclusion Phenom. Macrocyclic Chem.*, 2004, **49**, 133–137; (*c*) A. Cazacu, C. Tong, A. van der Lee, T. M. Fyles and M. Barboiu, *J. Am. Chem. Soc.*, 2006, **128**, 9541–9548; (*d*) M. Barboiu, S. Cerneaux, A. van der Lee and G. Vaughan, *J. Am. Chem. Soc.*, 2004, **126**, 3545–3550.

10 (*a*) A. Khaled, O. Piotrowska, K. Dominik and C. Augé, *Carbohydr. Res.*, 2008, **343**, 167–178; (*b*) M. Iwasaki, S. Inue and Y. Inue, *Eur. J. Biochem.*, 1987, **168**, 185–192; (*c*) D. M. Gray, J.-D. Wen, C. W. Gray, R. Repges, C. Repges, G. Raabe and J. Fleinschhauer, *Chirality*, 2008, **20**, 431–440.

11 For recent examples where CD was used to detect a G-quadruplex supramolecular assembly in a membrane, see: N. Sakai and S. Matile, *Chirality*, 2003, **15**, 766–771 and ref. 8*i*,*k*.

12 The Ba^{2+} G-quadruplex is thermodynamically and kinetically more stable than the K^{+} G-quadruplex. See: X. Shi, J. C. Fetiger and J. T. Davis, *J. Am. Chem. Soc.*, 2001, **123**, 6738–6739.